SciMedCentral

JSM Ophthalmology

Research Article

Effect of Corneal, Scleral and Lamina Cribrosa Elasticity, and Intraocular Pressure on Optic Nerve Damages

Match Wai Lun Ko*

Department of Mechanical Engineering, School of Engineering, Nazarbayev University, Kazakhstan

***Corresponding author**

Match W. L. Ko, Department of Mechanical Engineering, School of Engineering, Nazarbayev University, 53 Kabanbay Batyr Ave. Astana, 010000, Kazakhstan, Tel: 7-7172-709190, E-mail: matchkoust@gmail.com

Submitted: 04 December 2014

Accepted: 02 January 2015

Published: 04 January 2015

ISSN: 2333-6447

Keywords

- Glaucoma
- Optic nerve
- Computational modeling
- Intraocular pressure
- Ocular biomechanics
- Corneal elastic modulus
- Cornea

Abstract

Objectives: The aim of this study is to characterize the effect of corneal, scleral and lamina cribrosa (LC) elasticity, and intraocular pressure (IOP) on the optic nerve damages.

Methods: The effect of corneal, scleral and LC elasticity, and IOP on the shear stress in lamina cribrosa were modeled using computational finite element analysis. The nonlinear biomechanical properties of the corneal, scleral and LC were adapted from the literature and were varied to examine the effects of tissue biomechanical properties on the LC. The IOP were varied from 10 to 50 mmHg.

Results and discussion: The results showed that the shear stresses in LC increase with the corneal (E_c), scleral (E_s) and LC (E_{LC}) modulus, and IOP. Vision loss is determined by the Classical Tresca shear failure criterion. Nerve is classified as damage and vision is classified as lost when the shear stress in an optic nerve fiber along the thickness direction exceeds the Tresca critical damage shear stress. The results showed that nerve damage increases with the elastic moduli and IOP. The percentage nerve damage at 25 mmHg showed a logarithmic increase from 12.5% to 45.7% with the corneal elastic modulus increase from 0.17 MPa to 1.43MPa.The eyes with higher ocular elastic moduli (E_c, E_s and E_{LC}) are more sensitive to nerve damages from elevated IOP. The higher magnitude of ocular elastic moduli themselves does not introduce optic nerve damage but it would amplify the effect of IOP induced nerve damages by amplifying the shear stress in the LC.

Conclusion: The finding of optic nerve damage increases with ocular elastic moduli implies that, the clinical general screening guidance for glaucoma development risk assessment based on the IOP is not enough. The parameter of ocular elasticity should also include in the diagnosis stage. The corneal elasticity can be clinically assessed by various available medical devices like, Ocular Response Analyzer (ORA) and Corneal Visualization with Scheimpflug Technology (Corvis ST), while the clinical measurement of scleral and LC elasticity are currently impossible due to the lack of instruments. The corneal elasticity may be used as an independent parameter or to form a combined parameter with IOP, for the risk assessment of glaucoma development and progression.

INTRODUCTION

The eyes are one of our most important sensory organs and the eyes are specialized for the conversion of light into electrochemical signals. Ocular biomechanics play an important role in a significant number of ophthalmic pathologies. Corneal biomechanics is closely related to keratoconus [1] and glaucoma [2], scleral and lamina cribrosa (LC) biomechanics are a contributor to myopia [3] and glaucoma [4]. Material elasticity is a measure of how a material deforms in response to an external stress and literature regarding *ex vivo* study has shown that the ocular tissue exhibits non linear stress strain behavior such that the elastic angent modulus increases with increasing stress/intraocular pressure [5-11]. The stress strain curve for a nonlinear elastic material is nonlinear and tangent modulus, a measure of the instantaneous rate of change at a specific stress on the nonlinear stress strain curve, should be used instead of the Young's modulus as a property descriptor of the nonlinear elastic behavior over different stresses (pressures) [12]. The nonlinear behavior of ocular tissue to stress requires a nonlinear structural model that can capture the stiffening induced by the stress at high strains. Optic neuropathy in glaucoma can cause visual field loss and blindness [13,14]. Intraocular pressure (IOP) is one of the major risk factor of glaucoma and used as a screening parameter

for diagnosis in clinics. High IOP can cause glaucomatous damage to the optic nerves in the LC [15-18]. From experiments on human cadaver eyes, it is found that elevated IOP can lead to bowing of the LC and the axonal bundles of the optic nerve in the LC are sheared and disrupted under high IOP [15]. From the literature, computational models have been used to understand the biomechanical linkage between IOP and glaucoma [19-24]. Out of a number of structural and geometrical parameters selected, the scleral stiffness is identified to have the greatest influence on the optic nerve head (ONH) and the strains in the LC [20]. These results indicated that the biomechanical property of the sclera is a crucial factor that can affect the LC and that may be a reason that glaucoma patients were found to have higher ocular rigidity [25]. However, all the study on the biomechanical linkage between IOP and glaucoma focus on the sclera and ONH, none of them consider the influence of the corneal biomechanics and geometries into the modeling and analysis. Johnson *et al.* shows that the corneal elastic properties may serve a buffering mechanism to the micro volumetric change in the eye from the IOP [2]. The greater the corneal elasticity, the more protection to the eye from IOP surges. The greater elasticity may provide a larger buffer to sustain the fluctuation and evaluation of IOP [2]. Central corneal thickness, one of the corneal geometrical factors, has been shown to play a role in the interpretation of IOP and has also been suggested as a glaucoma risk factor [26]. Even though the cornea is far always from the primary site of glaucoma, lamina cribrosa (LC) of the sclera, the corneal biomechanics is still contributed to the ocular rigidity as a whole to protect the eye from the momentary IOP surges. However, a detail understanding of the change in corneal biomechanics to the risk of glaucoma development and progression remains to be determined. In this work, finite element modeling is used to quantify IOP-induced shear stresses within the LC. The aim of this study is to characterize the effect between the corneal, scleral and LC elasticity, and intraocular pressure on the optic nerve damages.

MATERIALS AND METHODS

Finite element (FE) modeling method was used to examine the influence of corneal, scleral and lamina cribrosa elasticity on the shear stress in LC. A 3-dimensional eyeball model (Figure 1) was built in a computer aided design (CAD) software (Solid works 2010, Das sault Systèmes Solid works Corp., MA, USA), and the model was then transferred to a FEA software (ANSYS 12.0.1, ANSYS, Inc., PA, USA) for computation. The model was adapted from Leung *et al.* [19] and the core structural dimensions of the model were adapted from Signal's study [20,21]. The thickness of the scleral, retina ,LC and pia mater, internal radius of globe, LC anterior surface central deflection and the dimensions and shape of pre laminar neural tissue were adapted from Signal's study [20]. The adipose tissue was assumed to be axisymmetric about the central axis of the LC and was set to cover 140 degrees of the globe. The thickness and elastic modulus of the adipose tissues was set to 4.6 mm and 0.047 MPa [27-29]. The corneal geometries were set to mean population value of 550μm (central corneal thickness) [30], 7.8 mm (corneal radius of curvature) [30,31] and 11 mm (corneal diameter) [32], respectively. The optic disc diameter and cup to disc ratio were set to 1.8 mm and 0.45, respectively [33]. The blind spot is around 15 degrees nasally from the fovea [34], so the angle between the central axis of cornea and that of the ONH region was set to 165 degrees. The coverage angle of pre laminar neural tissue was set to 80 degrees [20]. The elastic modulus of pia mater, pre and post laminar neural tissue were set to 3 MPa, 0.03 MPa and 0.03 MPa [20], respectively. The Poisson's ratio of all ocular tissues was set to 0.49 since it is practically incompressible [20,35].The ocular

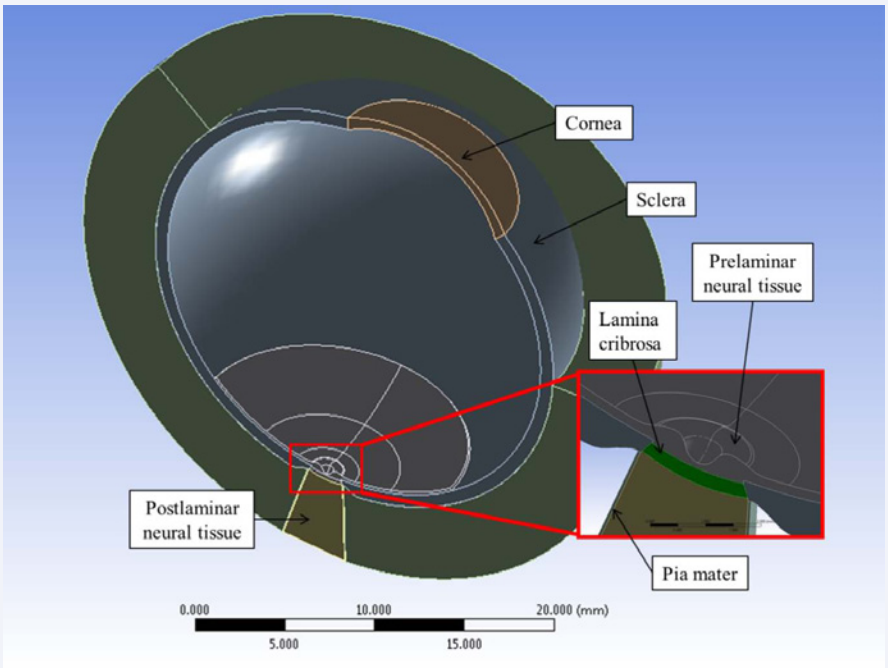

Figure 1 Three dimensional FEM eyeball model used in this study. The ocular geometries and material properties used in the FE model are detailed in (Table 1).

geometries and biomaterial properties used in the FE model were shown in (Table 1).

The IOP exerted on the inner surface of pre laminar neural tissue and the sclera by the vitreous body, and the inner surface of cornea by the aqueous humor were simulated by applying normal pressure loads onto the inner surfaces of eye. The IOP was varied from 10 to 50 mmHg with 5 mmHg interval. Coarse meshing of the structure was auto generated by the FEA software. The mesh in the ONH region was manually refined until the outputs have <0.5% differences even when the mesh density was doubled. The numerical accuracy was comparable to Leung's and Signal's study[19,20]. The nonlinear biomechanical properties of the corneal, scleral and LC were adapted from Woo's study [7] (Figure 2). To examine the effects of tissue biomechanical properties on the LC, the corneal, scleral and LC elastic moduli were varied under different IOPs (Table 2). The corneal elastic modulus (E_c) was varied from 0.17 to 1.43 MPa, the scleral elastic modulus (E_s) was varied from 1.84 to 3.72 MPa and the elastic modulus of the lamina cribrosa (E_{LC}) was varied from 0.12 to 0.67MPa, respectively.

RESULTS AND DISCUSSION

The distribution of shear stresses in LC from at 25mmHg is shown in (Figure 3). Glaucomatous vision loss from the periphery and progresses toward the center [34,36] and the optic nerve damage are shown to be sheared [15,37]. The distribution of shear stresses in LC from the computational model showed that the local shear stresses were highest at the peripheral anterior surface and lowest in the central anterior surface as shown in (Figure 3), which is consistent with the literature [19,34,36] and the shear stress based model is able to describe the general observation of glaucomatous vision loss.

The magnitude of shear stresses in LC was increased with the elastic modulus of ocular tissue as shown in (Figure 3). Since the corneal, scleral and LC elasticity varied together as shown in (Table 1), corneal elastic modulus was taken to represent the variation of the set of ocular elastic modulus. The effect of corneal tangent modulus on the maximum shear stresses in LC is shown

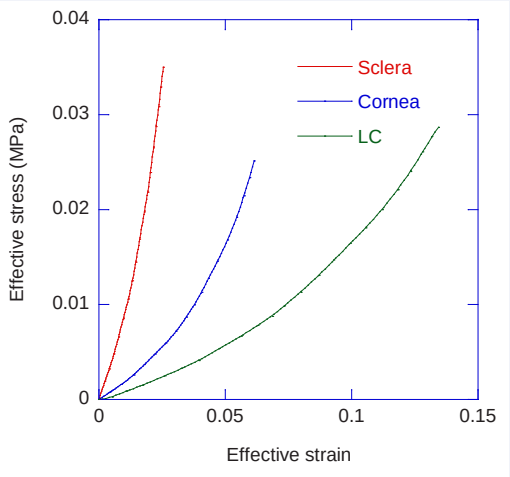

Figure 2 The nonlinear effective stress – effective strain curve for cornea scleral and LC adapted from Woo's study [7].

Table 1: Summary of the ocular geometries and biomaterial properties used in the eyeball FE model.

Parameters	Unit	Value	References
Internal radius of the globe	mm	12.0	[20]
Scleral thickness of the globe	mm	0.8	[20]
Scleral thickness closed to LC	mm	0.4	[20]
LC central thickness	mm	0.3	[20]
Retinal thickness	mm	0.2	[20]
Pia mater thickness	mm	0.06	[20]
Central corneal thickness	μm	550	[30]
Corneal radius of curvature	mm	7.8	[30, 31]
Corneal diameter	mm	11	[32]
LC anterior surface diameter	mm	1.9	[20]
LC anterior surface central deflection	mm	0.10	[20]
Cup depth	mm	0.33	[20]
Peripapillary rim height	mm	0.3	[20]
Optical disc diameter	mm	1.8	[33]
Optic nerve angle	degree	80	[20]
Canal wall angle to the horizontal	degree	60	[20]
Cup to disc ratio	—	0.45	[33]
Poisson ratio of all materials	—	0.49	[20, 35]
Elastic modulus of adipose tissue	MPa	0.047	[27-29]
Elastic modulus of pia mater	MPa	3	[20]
Elastic modulus of prelaminar neural tissue	MPa	0.03	[20]
Elastic modulus of postlaminar neural tissue	MPa	0.03	[20]

Table 2: The configuration set of corneal, scleral and LC elastic modulus.

	Elastic modulus (MPa)		
Set	Cornea	Sclera	LC
1	0.17	1.84	0.12
2	0.31	2.05	0.21
3	0.45	2.26	0.27
4	0.59	2.47	0.32
5	0.73	2.68	0.38
6	0.87	2.88	0.44
7	1.01	3.09	0.50
8	1.15	3.30	0.55
9	1.29	3.51	0.61
10	1.43	3.72	0.67

in (Figure 4). The plots showed that the maximum shear stresses in LC (τ_{max}) increase with the increase of corneal elastic modulus and IOP. The τ_{max} increases with corneal elastic modulus even at the same IOP and τ_{max} is more sensitive to the change in IOP than the change in corneal elastic modulus. The maximum shear stress in LC is not only dependent on IOP, but also the corneal elastic modulus. Vision loss is determined by classical Tresca shear failure criterion (maximum shear stress failure criterion) [19, 38-41]. Experimental evident showed that the optic nerves were

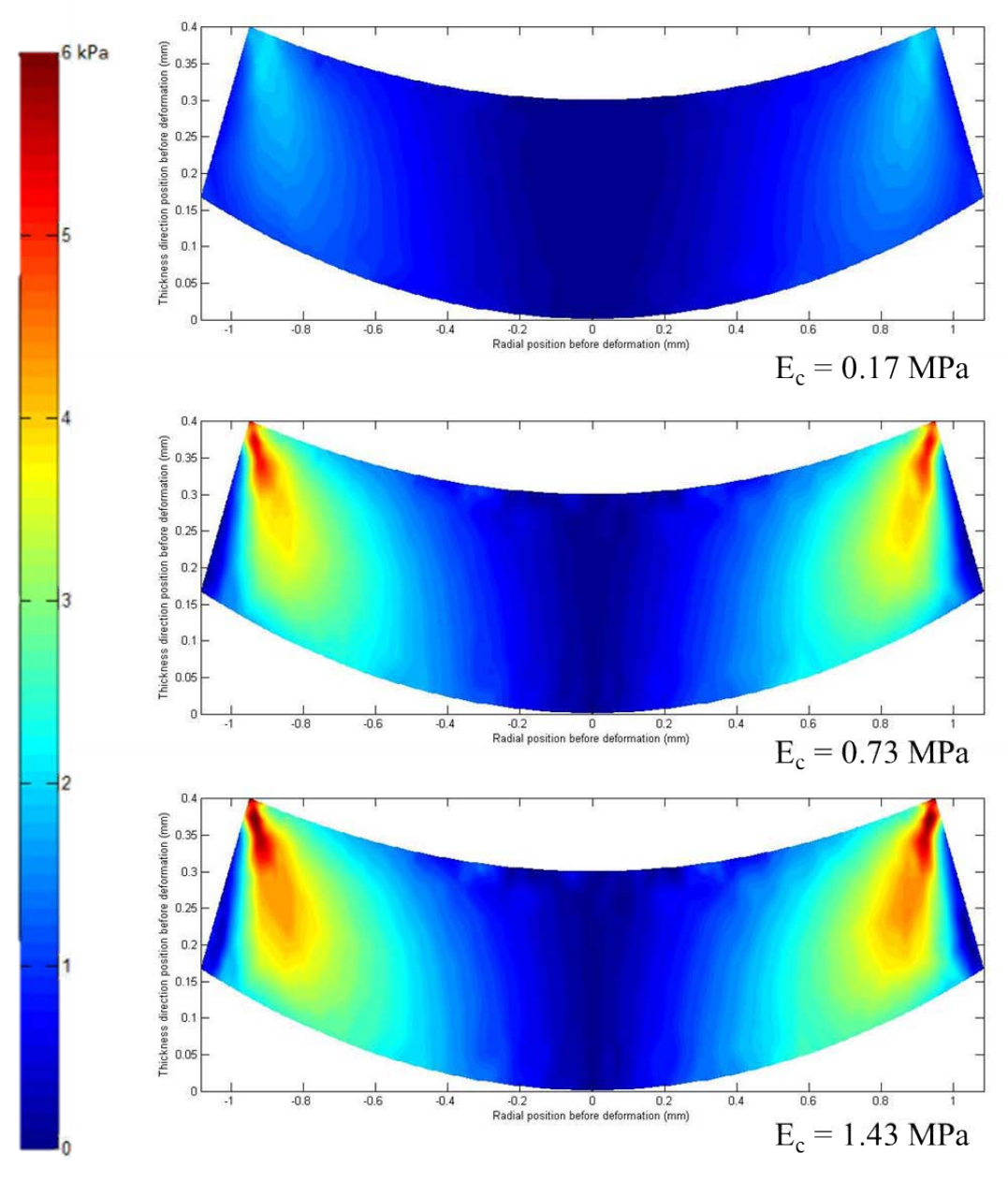

Figure 3 Shear stress distribution in the diametrical cross section of the LC for IOP equal to 25 mmHg.

damaged by shear [15] and the Tresca shear failure criterion was shown to be capable to reasonably predict the nerve damage behavior. The vision of a particular optic nerve is lost when the corresponding optic nerve is damaged. Nerve is classified as damaged and vision is classified as lost when the shear stress in an optic nerve fiber along the thickness direction (τ_a) exceeds the Tresca critical damage shear stress (τ_c), i.e., $\tau_a \geq \tau_c$. The maximum shear stresses along the thickness direction in the LC (τ_{max}) were determined from the model. The nerve damage criterion is implemented as follow,

$$Nerve = \begin{cases} Damaged, & \tau_{\max} \geq \tau_c \\ Not\ damaged, & \tau_{\max} < \tau_c \end{cases} \quad (1)$$

Ocular hypertension refers to a situation that the IOP is greater than 21 mmHg and no optic nerve damage and vision loss are present. The nerve damage in normal eye is negligible statistically, so a τ_c of 0.0035 MPa is taken so that the τ_{max} (0.0032 MPa) in normal eyes (E_c = 0.17 MPa, E_s = 1.84 MPa and E_{LC} = 0.12 MPa) under IOP of 20mmHg does not exceed τ_c. Using the criterion, the optic nerve damages for eyes under different ocular elasticity configurations and IOPs were estimated and are shown in (Figure 5). The results showed that the nerve damage increases with the corneal tangent modulus and IOP. The nerve damage increases with E_c even at the same IOP. Although the nerve damage is more sensitive to the change in IOP than the change in E_c, the percentage nerve damage at 25 mmHg IOP increased logarithmically from 12.5% to 45.7% with the corneal tangent modulus increased from 0.17 MPa to 1.43MPa.The eyes with

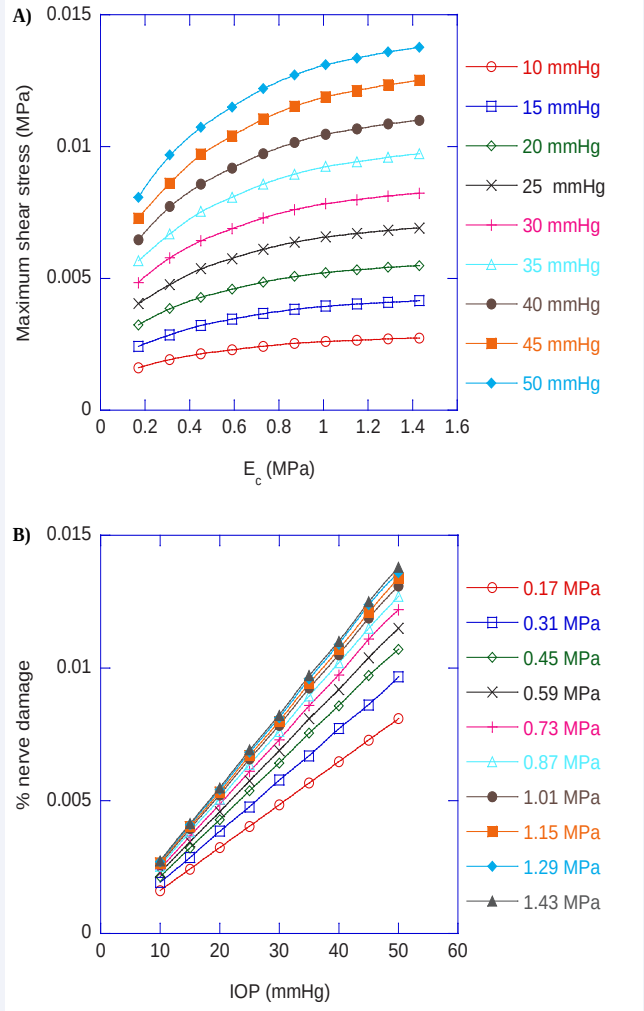

Figure 4 (a) Maximum shear stresses in the LC as a function of Ec with IOP varied from 10 to 50 mmHg. (b) Maximum shear stresses in the LC as a function of IOP with Ec varied from 0.17to 1.43 MPa.

higher ocular elastic moduli (E_c, E_s and E_{LC}) are more sensitive to nerve damages from elevated IOP. The higher ocular moduli itself does not introduce optic nerve damage but it could amplify the effect of the IOP induced nerve damages by amplifying the shear stresses in LC. The ocular elasticity is known to be stiffened with age [42-46] and that's mean the older population with stiffened ocular elasticity would be more susceptible to vision loss due to the amplified shear stresses in LC. Elderly are expected to have higher risk to glaucoma development and progression and this population should be monitored more frequently than people with normal ocular elasticity. The susceptibility of an eye to glaucomatous damage is affected not only by the IOP, but also the ocular biomechanical properties. In order to identify the people at high risk of glaucoma development and progression, clinical diagnostic methods can be developed based on the characterization of the ocular tissue elasticity *in vivo*. Since the sclera and LC are embedded in the eye and there is no available method for the *in vivo* characterization of the scleral and LC elasticity, the characterization and monitoring of the corneal elastic modulus is the only solution. Several *in vivo* corneal measurements were developed, including the opto mechanical testing device [47], mechanical indentation testing device [8,48], air jet indentation testing device with optical coherence tomography [49,50], high frequency ultrasound elasticity microscope [51,52], novel scanning acoustic microscopy [53], confocal Brillouin microscopy [54], Ocular Response Analyzer (ORA; Reichert, Corp., Buffalo, NY) [55] and Corneal Visualization with Scheimpflug Technology (Corvis ST; Oculus Inc., Wetzlar, Germany) [56,57]. With the utilization of available corneal elasticity measurement methodologies, further clinical studies can then be performed to examine the potential use of corneal elasticity in glaucoma risk assessment and disease treatment management. The current study agreed with the current understanding that the optic nerve head biomechanics and optic nerve damage are strongly dependent on the scleral biomechanical properties [4,20-24]. The current study used a whole eye model to simulate the LC behavior under different ocular tissue elasticity and IOPs, added the linkage between the corneal biomechanics and the optic nerve damage and proposed the corneal elasticity as an indirect measurement of glaucoma risk. In the current study, we considered only the biomechanical properties variation of the ocular tissue to the optic nerve

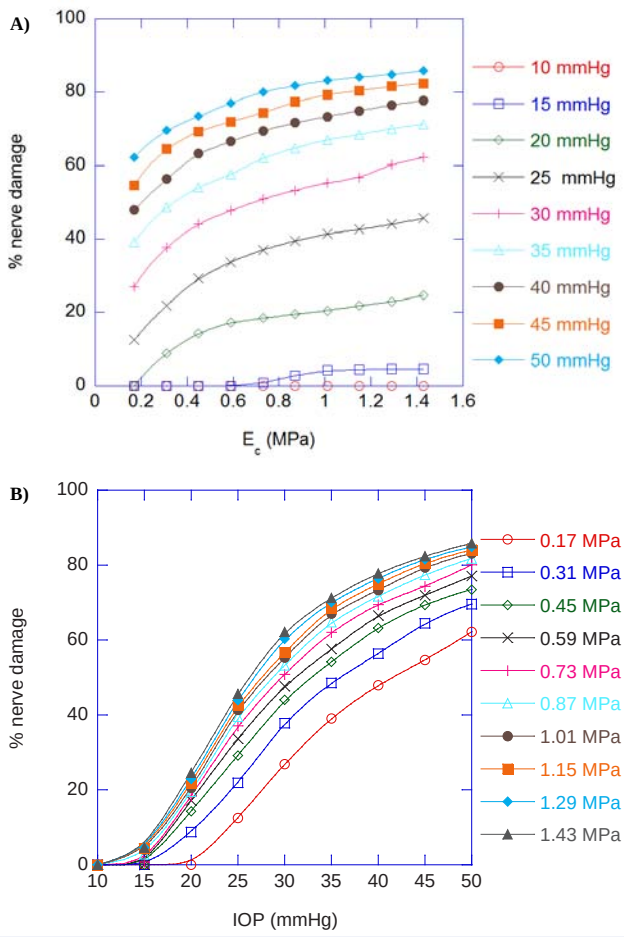

Figure 5 (a) Nerve damage as a function of Ec with IOP varied from 10 to 50 mmHg.
(b) Nerve damage as a function of IOP with Ec varied from 0.17to 1.43 MPa.

damage but ignore the other glaucomatous optic neuropathy. The ocular structure was also greatly simplified in order to simplify the modeling and analysis. In the current ocular model, only core load bearing structure was considered. The ocular tissue properties are generally viscoelastic and the ocular response are time dependent. However, in the current model, we followed the literature using elastic modeling approach for analysis [21,22]. Refinement of the model can be incorporated with ocular tissue data from ex vivo animal and clinical human data, and nonlinear viscoelastic modeling.

CONCLUSION

This finding implies that, the clinical general screening guidance for the risk assessment of glaucoma based on the IOP is not enough. The parameter of corneal, scleral and LC elasticity should include also in the diagnosis stage. The corneal elasticity can be clinically assessed by various commercially available medical devices, while the clinical measurement of scleral and LC elasticity are currently impossible due to the lack of instruments. The corneal elasticity maybe used as an independent parameter or to form a combined parameter with IOP for the risk assessment of glaucoma development and progression.

REFERENCES

1. Andreassen TT, Hjorth Simonsen A, Oxlund H. Biomechanical properties of keratoconus and normal corneas. Experimental eye research. 1980; 31: 435-441.
2. Johnson C, Mian S, Moroi S, Epstein D, Izatt J, Afshari N. Role of corneal elasticity in damping of intraocular pressure. Investigative ophthalmology & visual science. 2007; 48: 2540-2544.
3. McBrien NA, Jobling AI, Gentle A. Biomechanics of the sclera in myopia: extracellular and cellular factors. Optometry & Vision Science. 2009; 86: 23-30.
4. Sigal IA, Ethier CR. Biomechanics of the optic nerve head. Experimental eye research. 2009; 88: 799-807.
5. Boote C, Dennis S, Huang Y, Quantock A, Meek K. Lamellar orientation in human cornea in relation to mechanical properties. Journal of structural biology. 2005; 149: 1-6.
6. Coudrillier B, Tian J, Alexander S, Myers KM, Quigley HA, Nguyen TD. Biomechanics of the human posterior sclera: age-and glaucoma-related changes measured using inflation testing. Investigative ophthalmology & visual science. 2012; 53: 1714-1728.
7. Woo S, Kobayashi A, Schlegel W, Lawrence C. Nonlinear material properties of intact cornea and sclera. Experimental eye research. 1972; 14: 29-39.
8. Ko MWL, Leung LKK, Lam DCC, Leung CKS. Characterization of corneal tangent modulus in vivo. Acta Ophthalmologica. 2013; 91: 263-269.
9. Hoeltzel DA, Altman P, Buzard K, Choe K. Strip extensiometry for comparison of the mechanical response of bovine, rabbit, and human corneas. Journal of biomechanical engineering. 1992; 114: 202-215.
10. Elsheikh A, Alhasso D, Rama P. Biomechanical properties of human and porcine corneas. Experimental Eye Research. 2008; 86: 783-790.
11. Leung LKK, Ko MWL, Ye C, Lam DCC, Leung CKS. Non-invasive measurement of scleral stiffness and tangent modulus in porcine eyes. Investigative ophthalmology & visual science. 2014; 55: 3721-3726.
12. Buzard K. Introduction to biomechanics of the cornea. Refractive & corneal surgery. 1992; 8: 127-138.
13. Weinreb RN, Shakiba S, Sample PA, Shahrokni S, Van Horn S, Garden VS, et al. Association between quantitative nerve fiber layer measurement and visual field loss in glaucoma. American journal of ophthalmology. 1995; 120: 732-738.
14. Katz J, Gilbert D, Quigley HA, Sommer A. Estimating progression of visual field loss in glaucoma. Ophthalmology. 1997; 104: 1017-1025.
15. Yan DB, Coloma FM, Metheetrairut A, Trope GE, Heathcote JG, Ethier CR. Deformation of the lamina cribrosa by elevated intraocular pressure. British Journal of Ophthalmology. 1994; 78: 643-648.
16. Azuara-Blanco A, Costa VP, Wilson RP. Handbook of glaucoma: Informa HealthCare; 2001.
17. Anderson DR, Hendrickson A. Effect of intraocular pressure on rapid axoplasmic transport in monkey optic nerve. Investigative ophthalmology & visual science. 1974; 13: 771-783.
18. Quigley H, Broman A. The number of people with glaucoma worldwide in 2010 and 2020. British Journal of Ophthalmology. 2006; 90: 262-267.
19. Leung LKK, Ko MWL, Lam DCC. Effect of Age-Stiffening Tissues and Intraocular Pressure on Optic Nerve Damages. MCB: Molecular & Cellular Biomechanics. 2012; 9: 157-174.
20. Sigal IA, Flanagan JG, Ethier CR. Factors influencing optic nerve head biomechanics. Investigative ophthalmology & visual science. 2005; 46: 4189-4199.
21. Sigal IA, Flanagan JG, Tertinegg I, Ethier CR. Finite element modeling of optic nerve head biomechanics. Investigative ophthalmology & visual science. 2004; 45: 4378-4387.
22. Burgoyne CF, Downs JC, Bellezza AJ, Francis Suh JK, Hart RT. The optic nerve head as a biomechanical structure: a new paradigm for understanding the role of IOP-related stress and strain in the pathophysiology of glaucomatous optic nerve head damage. Progress in retinal and eye research. 2005; 24: 39-73.
23. Girard MJ, Downs JC, Burgoyne CF, Suh J-KF. Peripapillary and posterior scleral mechanics—part I: development of an anisotropic hyperelastic constitutive model. Journal of biomechanical engineering. 2009; 131.
24. Girard MJ, Downs JC, Bottlang M, Burgoyne CF, Suh J-KF. Peripapillary and posterior scleral mechanics—part II: experimental and inverse finite element characterization. Journal of biomechanical engineering. 2009; 131.
25. Ebneter A, Wagels B, Zinkernagel M. Non-invasive biometric assessment of ocular rigidity in glaucoma patients and controls. Eye. 2009; 23: 606-611.
26. Herndon LW, Weizer JS, Stinnett SS. Central corneal thickness as a risk factor for advanced glaucoma damage. Archives of ophthalmology. 2004; 122: 17-21.
27. Bidar M, Ragan R, Kernozek T, Matheson JW. Finite element calculation of seat-interface pressures for various wheelchair cushion thicknesses. Chicago, Illinois. 2000.
28. Todd BA, Thacker JG. Three-dimensional computer model of the human buttocks in vivo. Journal of Rehabilitation Research and Development. 1994; 31: 111-119.
29. Power ED. A nonlinear finite element model of the human eye to investigate ocular injuries from night vision goggles: Virginia Polytechnic Institute and State University; 2001.
30. Shimmyo M, Ross AJ, Moy A, Mostafavi R. Intraocular pressure, Goldmann applanation tension, corneal thickness, and corneal curvature in Caucasians, Asians, Hispanics, and African Americans. American journal of ophthalmology. 2003; 136: 603-613.

31. Bier N, Lowther G. Contact lens correction: Butterworth-Heinemann; 1977.

32. Ren R, Wang N, Li B, Li L, Gao F, Xu X, et al. Lamina cribrosa and peripapillary sclera histomorphometry in normal and advanced glaucomatous Chinese eyes with various axial length. Investigative ophthalmology & visual science. 2009; 50: 2175-2184.

33. Sing T, Noelani M, Anderson S, Townsend J. The normal optic nerve head. Optometry & Vision Science. 2000; 77: 293-301.

34. Allingham RR, Shields MB, Damji KF, Freedman S, Moroi SE, Shafranov G. Shields' textbook of glaucoma: Lippincott Williams & Wilkins. 2005.

35. Kampmeier J, Radt B, Birngruber R, Brinkmann R. Thermal and biomechanical parameters of porcine cornea. Cornea. 2000; 19: 355-363.

36. Drance SM. The glaucomatous visual field. British Medical Journal. 1972; 56: 186-200.

37. Edwards ME, Steven SSW, Good TA. Role of viscoelastic properties of differentiated SH-SY5Y human neuroblastoma cells in cyclic shear stress injury. Biotechnology progress. 2008; 17: 760-767.

38. Yu M. Unified strength theory and its applications: Springer; 2004.

39. Tresca HE. Memoire sur l'ecoulement des corps solides soumis a de fortes pressions: Gauthier-Villars; 1864.

40. Gardiner JC, Weiss JA. Simple shear testing of parallel-fibered planar soft tissues. Journal of biomechanical engineering. 2001; 123: 170-175.

41. Ionescu I, Guilkey JE, Berzins M, Kirby RM, Weiss JA. Simulation of soft tissue failure using the material point method. Journal of biomechanical engineering. 2006; 128: 917-924.

42. Elsheikh A, Geraghty B, Rama P, Campanelli M, Meek KM. Characterization of age-related variation in corneal biomechanical properties. Journal of the Royal Society Interface. 2010; 7: 1475-1485.

43. Geraghty B, Jones SW, Rama P, Akhtar R, Elsheikh A. Age-related variations in the biomechanical properties of human sclera. Journal of the mechanical behavior of biomedical materials. 2012; 16: 181-191.

44. Albon J, Purslow PP, Karwatowski WSS, Easty DL. Age related compliance of the lamina cribrosa in human eyes. British Journal of Ophthalmology. 2000; 84: 318-323.

45. Friberg TR, Lace JW. A comparison of the elastic properties of human choroid and sclera. Experimental Eye Research. 1988; 47: 429-436.

46. Cartwright NEK, Tyrer JR, Marshall J. Age-related differences in the elasticity of the human cornea. Investigative ophthalmology & visual science. 2011; 52: 4324-4329.

47. Chang S, Hjortdal J, Maurice D, Pinsky P. Corneal deformation by indentation and applanation forces. Investigative ophthalmology & visual science. 1993; 34: 1241.

48. Ko MWL, Leung LKK, Lam DCC. Comparative study of corneal tangent elastic modulus measurement using corneal indentation device. Medical engineering & physics. 2014; 36: 1115-1121.

49. Ko MWL, Wang LK, Zhang JY, Li TJ, Tian L, Zheng YP. Corneal biomechanical properties characterization using Air-jet Indentation based Optical Coherence Tomography (AIOCT) system. Medical engineering & physics. 2014.

50. Alonso-Caneiro D, Karnowski K, Kaluzny BJ, Kowalczyk A, Wojtkowski M. Assessment of corneal dynamics with high-speed swept source optical coherence tomography combined with an air puff system. Optics express. 2011; 19: 14188-14199.

51. Tanter M, Touboul D, Gennisson J-L, Bercoff J, Fink M. High-resolution quantitative imaging of cornea elasticity using supersonic shear imaging. Medical Imaging, IEEE Transactions on. 2009; 28: 1881-1893.

52. Hollman KW, Shtein RM, Tripathy S, Kim K. Using an ultrasound elasticity microscope to map three-dimensional strain in a porcine cornea. Ultrasound in medicine & biology. 2013; 39: 1451-149.

53. Beshtawi IM, Akhtar R, Hillarby MC, O'Donnell C, Zhao X, Brahma A, et al. Biomechanical properties of human corneas following low- and high-intensity collagen cross-linking determined with scanning acoustic microscopy. Investigative ophthalmology & visual science. 2013; 54: 5273-5280.

54. Scarcelli G, Pineda R, Yun SH. Brillouin optical microscopy for corneal biomechanics. Investigative ophthalmology & visual science. 2012; 53: 185-190.

55. Luce DA. Determining in vivo biomechanical properties of the cornea with an ocular response analyzer. Journal of Cataract & Refractive Surgery. 2005; 31: 156-162.

56. Ambrósio Jr R, Caldas DL, Ramos IC, Santos R, Belin M, editors. Corneal Biomechanical Assessment Using Dynamic Ultra High-Speed Scheimpflug Technology Non-contact Tonometry (UHS-ST NCT): Preliminary Results. American Society of Cataract and Refractive Surgery-American Society of Ophthalmic Administrators (ASCRS-ASOA) Symposium and Congress San Diego, CA; 2011.

57. Tian L, Ko MWL, Wang LK, Zhang JY, Li TJ, Huang YF, et al. Assessment of ocular biomechanics using dynamic ultra high-speed scheimpflug imaging in keratoconic and normal eyes. Journal of refractive surgery (Thorofare, NJ: 1995). 2014; 30: 785-791.

Cite this article

Ko MWL (2015) Effect of Corneal, Scleral and Lamina Cribrosa Elasticity, and Intraocular Pressure on Optic Nerve Damages. JSM Ophthalmol 3(1): 1024.